

Electromagnetic form factors at large momenta from lattice QCD

A. J. Chambers,¹ J. Dragos,^{1,2} R. Horsley,³ Y. Nakamura,⁴ H. Perlt,⁵ D. Pleiter,^{6,7} P. E. L. Rakow,⁸
G. Schierholz,⁹ A. Schiller,⁵ K. Somfleth,¹ H. Stüben,¹⁰ R. D. Young,¹ and J. M. Zanotti¹

(QCDSF/UKQCD/CSSM Collaborations)

¹*CSSM, Department of Physics, University of Adelaide, Adelaide SA 5005, Australia**

²*National Superconducting Cyclotron Laboratory and Department of Physics and Astronomy,
Michigan State University, East Lansing, MI 48824, USA*

³*School of Physics and Astronomy, University of Edinburgh, Edinburgh EH9 3JZ, UK*

⁴*RIKEN Advanced Institute for Computational Science, Kobe, Hyogo 650-0047, Japan*

⁵*Institut für Theoretische Physik, Universität Leipzig, 04103 Leipzig, Germany*

⁶*JSC, Jülich Research Centre, 52425 Jülich, Germany*

⁷*Institut für Theoretische Physik, Universität Regensburg, 93040 Regensburg, Germany*

⁸*Theoretical Physics Division, Department of Mathematical Sciences,
University of Liverpool, Liverpool L69 3BX, UK*

⁹*Deutsches Elektronen-Synchrotron DESY, 22603 Hamburg, Germany*

¹⁰*Regionales Rechenzentrum, Universität Hamburg, 20146 Hamburg, Germany*

Accessing hadronic form factors at large momentum transfers has traditionally presented a challenge for lattice QCD simulations. Here we demonstrate how a novel implementation of the Feynman–Hellmann method can be employed to calculate hadronic form factors in lattice QCD at momenta much higher than previously accessible. Our simulations are performed on a single set of gauge configurations with three flavours of degenerate mass quarks corresponding to $m_\pi \approx 470$ MeV. We are able to determine the electromagnetic form factors of the pion and nucleon up to approximately 6 GeV², with results for G_E/G_M in the proton agreeing well with experimental results.

PACS numbers: 12.38.Gc, 14.20.Dh

I. INTRODUCTION

One of the great challenges of hadron physics is to build consistent and informative pictures of the internal structures of strongly-interacting particles. An important aspect of this endeavour is the calculation of electromagnetic form factors for various baryons and mesons. These encode a description of the distribution of electromagnetic currents in hadrons and are key to describing the extended structure of these composite states.

For most of the second half of the 20th century, measurements of the electromagnetic form factors of the nucleon were obtained using the Rosenbluth separation technique [1] (also e.g. [2]). Broadly, these experiments indicated that the electric and magnetic form factors scaled proportionally for Q^2 up to around 6 GeV², with $\mu_p G_{E_p}/G_{M_p} \approx 1$. This was later found to be in disagreement with recoil polarisation experiments at Jefferson Lab which showed $\mu_p G_{E_p}/G_{M_p}$ decreasing approximately linearly for $Q^2 \gtrsim 0.5$ GeV² (see e.g. [3–7]). This discrepancy is now largely understood through studies of two-photon exchange effects in the Rosenbluth method [8, 9]. Nevertheless, it is still unknown whether the linear Q^2 trend continues and crosses zero, or if the fall-off with Q^2 slows down. Experimental results are as yet unable to obtain precise results at the relevant momentum scales, and so this remains an open question.

Resolving the scaling of the form factors in this domain is one of the key physics goals of the upgraded CEBAF at Jefferson Lab.

The large- Q^2 behaviour of the pion electromagnetic form factor F_π has proven challenging to probe experimentally — see Refs. [10–12] for recent innovative advances. Besides providing information about the electromagnetic structure of the pion, the Q^2 -behaviour of F_π provides insight into the transition from the soft to the hard regime in QCD (see [13] for a recent example). Owing to the present limitations, experimental data are unable to reliably discriminate different models describing the transition to the asymptotic domain [14].

Lattice calculations of hadronic form factors have typically focussed on the study of processes at low-momentum transfer (see e.g. [15–20]), with only limited studies at large $Q^2 \gtrsim 3$ GeV² [21, 22]. There are a variety of reasons that have contributed to the difficulty in accessing high-momentum transfer in lattice QCD. Given that the form factors fall with Q^2 , it is immediately clear that one is attempting to extract a much weaker signal from datasets obtained with finite statistics. Further, in terms of the numerical computation, the signal-to-noise ratio of hadron correlators rapidly deteriorates as the momentum of the state is increased. This had commonly led to the study of 3-point correlators which are projected to zero momentum at the hadron sink. In this case, the possible momentum transfers are limited by the maximum momentum available at the source. With limited statistical signal, it is therefore difficult to assess the de-

* alexander.chambers@adelaide.edu.au

gree of excited-state contamination, which can lead to significant systematic uncertainty [19, 21, 23–25].

In the present work we demonstrate the ability to access high-momentum transfer in hadron form factors on the lattice using an extension of the Feynman–Hellmann theorem to non-forward matrix elements. This builds upon recent applications of the Feynman–Hellmann theorem for hadronic matrix elements in lattice QCD [26–29] — see also Refs. [30–37] for similar related techniques. Through the Feynman–Hellmann theorem one relates matrix elements to energy shifts. In the case of lattice QCD this allows one to access matrix elements from 2-point correlators, rather than a more complicated analysis of 3-point functions. This greatly simplifies the process of neutralising excited-state contamination. As described below, the method most naturally works in the Breit frame ($E(\mathbf{p}') = E(\mathbf{p})$) and hence one maximises the momentum transfer for any given accessible state momentum $|\mathbf{p}|$. Finally, the high degree of correlations in the gauge ensembles makes it possible to extract a weak signal from a relatively noisy state.

II. FEYNMAN–HELLMANN METHODS

To extend the Feynman–Hellmann analysis to non-forward matrix elements, we first consider a simple quantum mechanical situation. The familiar form of the FH theorem reads

$$\frac{\partial E_\psi}{\partial \lambda} = \left\langle \psi \left| \frac{\partial H}{\partial \lambda} \right| \psi \right\rangle, \quad (1)$$

where E is the energy eigenvalue of the state ψ . This readily follows from first-order perturbation theory. In the presence of spatially-varying external fields, the conventional theorem requires a slight modification. We consider some first-order perturbation of the Hamiltonian, $H = H_0 + \lambda V$, which couples to a definite (real) spatial Fourier component

$$\frac{\partial H}{\partial \lambda} \equiv \tilde{V}_+(\mathbf{q}) = \tilde{V}(\mathbf{q}) + \tilde{V}(-\mathbf{q}), \quad (2)$$

defined in terms of the complex Fourier modes $\tilde{V}(\mathbf{q}) = \int d^3\mathbf{y} e^{i\mathbf{q}\cdot\mathbf{y}} V(\mathbf{y})$, for some Hermitian potential $V(\mathbf{y})$. The diagonal matrix elements of this operator vanish in the basis of definite momentum eigenstates

$$\langle \mathbf{p} | \tilde{V}_+(\mathbf{q}) | \mathbf{p} \rangle = 0, \quad (3)$$

and standard perturbation theory would suggest that there is no shift of the energy level at first order in λ . The exception to this rule is in the case of a degeneracy in the unperturbed eigenstates $E_0(\mathbf{p}) = E_0(\mathbf{p} \pm \mathbf{q})$. The familiar solution in this case is to invoke degenerate perturbation theory where one diagonalises the space of the degeneracy with respect to the applied external potential. The degeneracy condition dictates that one is considering

Breit-frame transitions. For demonstrative purposes, we choose the simple case where $\mathbf{p} = \pm\mathbf{q}/2$ and hence at lowest order in the field strength the system is diagonalised by the states $|\mathbf{q}/2\rangle_\pm \propto |\mathbf{q}/2\rangle \pm |-\mathbf{q}/2\rangle$. The corresponding eigenvalues are given by $E_0(\mathbf{q}/2) \pm \lambda\Delta E + \mathcal{O}(\lambda^2)$, where the energy shift corresponds to the matrix element of interest,

$$\Delta E = {}_+ \langle \mathbf{q}/2 | \tilde{V}_+(\mathbf{q}) | \mathbf{q}/2 \rangle_+ = \langle \mathbf{q}/2 | \tilde{V}(\mathbf{q}) | -\mathbf{q}/2 \rangle. \quad (4)$$

Owing to the discretised spectrum (and momentum) on the lattice, this quantum mechanical argument translates in a straightforward fashion to hadronic matrix elements. In the case of continuous momenta the presence of the periodic potential induces a gap in the dispersion curve, as in conventional band theory.

To implement within a lattice calculation, the Lagrangian is modified to incorporate a spatially-varying external potential

$$\mathcal{L}(y) \rightarrow \mathcal{L}(y) + \lambda \left(e^{+i\mathbf{q}\cdot\mathbf{y}} + e^{-i\mathbf{q}\cdot\mathbf{y}} \right) \mathcal{O}(y), \quad (5)$$

where the phase of the exponentials is defined with respect to the location of the hadron source at $\mathbf{y} = \mathbf{0}$. The symbol \mathcal{O} denotes a quark-bilinear operator and λ represents the strength of the external field — which is kept small ensure that the energy response is in the linear regime. Alternatively, one may isolate the linear λ dependence of the correlator directly by constructing compound propagators [36, 37].

To compute connected quark contributions, quark propagators are inverted according to the modified action corresponding to Eq. (5) — sea-quark contributions would require new gauge ensembles [29] or an effective reweighting technique. Fourier-projected, hadron correlation functions are defined by

$$C_{\mathbf{p}}^\lambda(t) = \sum_{\mathbf{x}} e^{-i\mathbf{p}\cdot\mathbf{x}} {}_\lambda \langle \Omega | \chi(t, \mathbf{x}) \chi^\dagger(0, \mathbf{0}) | \Omega \rangle_\lambda, \quad (6)$$

where subscript $|\Omega\rangle_\lambda$ is the vacuum of the modified theory. The spectrum can be directly isolated by constructing even and odd linear combinations,

$$C_{\mathbf{p},\mathbf{p}'}^{\lambda\pm} = C_{\mathbf{p}}^\lambda \pm C_{\mathbf{p}'}^\lambda, \quad (7)$$

of Breit-frame momentum pairs, \mathbf{p} and $\mathbf{p}' (= \mathbf{p} + \mathbf{q})$. To isolate an energy shift, it is more straightforward to implement the “+” combination $C_{\mathbf{p},\mathbf{p}'}^{\lambda+}$, rather than the “−” sum, which vanishes in the free-field limit.

Only the Breit-frame pairs will receive an energy shift which is linear in the applied field strength λ . This energy shift corresponds directly to the hadronic matrix element of interest

$$\left. \frac{\partial E_H(\mathbf{p}')}{\partial \lambda} \right|_{\lambda=0} = \frac{\langle H(\mathbf{p}') | \mathcal{O}(0) | H(\mathbf{p}) \rangle}{\langle H(\mathbf{p}') | H(\mathbf{p}') \rangle}, \quad (8)$$

or similarly for $\mathbf{p} \leftrightarrow \mathbf{p}'$. We have confirmed numerically that non-Breit frame states do not receive a linear energy response, as expected.

\mathbf{q}	\mathbf{p}	\mathbf{p}^2	Q^2
(0, 0, 0)	(0, 0, 0)	0	0
(2, 0, 0)	(1, 0, 0)	1	4
(2, 2, 0)	(1, 1, 0)	2	8
(2, 2, 2)	(1, 1, 1)	3	12
(4, 0, 0)	(2, 0, 0)	4	16
(4, 2, 0)	(2, 1, 0)	5	20
(4, 2, 2)	(2, 1, 1)	6	24

TABLE I. Momentum insertions and the corresponding Breit-frame momenta used in these calculations, where $\mathbf{p}' = -\mathbf{p}$. Momenta are given in lattice Fourier units of $2\pi/L$.

III. SIMULATION DETAILS

In the present work, we use an ensemble of 1700 gauge field configurations with $2 + 1$ flavours of non-perturbatively $O(a)$ -improved Wilson fermions and a lattice volume of $L^3 \times T = 32^3 \times 64$. The lattice spacing $a = 0.074(2)$ fm is set using a number of singlet quantities [38–41]. The clover action used comprises the tree-level Symanzik improved gluon action together with a stout smeared fermion action, modified for the implementation of the FH method [27].

We use a single ensemble with hopping parameters, $(\kappa_l, \kappa_s) = (0.120900, 0.120900)$, which correspond to a pion mass of ~ 470 MeV. To study electromagnetic form factors, quark propagators are calculated with the modified Lagrangian

$$\mathcal{L}(y) \rightarrow \mathcal{L}(y) + \left(e^{+i\mathbf{q}\cdot\mathbf{y}} + e^{-i\mathbf{q}\cdot\mathbf{y}} \right) \bar{q}(y) \lambda \cdot \gamma q(y), \quad (9)$$

for multiple values of \mathbf{q} as listed in Table I, where either λ_2 or λ_4 take non-zero values of 1×10^{-4} or -1×10^{-5} . Note that we only use the simplest Breit-frame kinematics, $\mathbf{p}' = -\mathbf{p}$. This choice allows us to minimise \mathbf{p}^2 for each value of \mathbf{q}^2 , and hence minimise the noise in the correlator. As described below, this also projects the nucleon energy shifts directly onto G_E or G_M .

IV. RESULTS

A. Electromagnetic Form Factors of the Nucleon

The (Euclidean) decomposition of the vector current for the individual quark flavour contributions of the nucleon is written in terms of the familiar Dirac and Pauli (F_{1q} and F_{2q}) form factors,

$$\langle N(p', s') | \bar{q}(0) \gamma_\mu q(0) | N(p, s) \rangle = \bar{u}(p', s') \left[\gamma_\mu F_{1q}(Q^2) + \frac{\sigma_{\mu\nu} q_\nu}{2M_N} F_{2q}(Q^2) \right] u(p, s), \quad (10)$$

where we denote the invariant 4-momentum transfer squared as $Q^2 = -q^2 = -(p' - p)^2$. The Sachs elec-

tromagnetic form factors are defined by

$$G_{E_q} = F_{1q} - \frac{Q^2}{(2M)^2} F_{2q} \quad (11)$$

$$G_{M_q} = F_{1q} + F_{2q} \quad (12)$$

For the incident-normal Breit frame ($\mathbf{p}' = -\mathbf{p}$), the temporal and spatial components of the current give rise to energy shifts which directly project out the electric and magnetic form factors respectively,

$$\left. \frac{\partial E_N}{\partial \lambda_4} \right|_{\lambda=0}^{\mathbf{p}' = -\mathbf{p}} = \frac{M_N}{E_N} G_{E_q}, \quad (13)$$

$$\left. \frac{\partial E_N}{\partial \lambda_i} \right|_{\lambda=0}^{\mathbf{p}' = -\mathbf{p}} = \frac{[\hat{\mathbf{e}} \times \mathbf{q}]_i}{2E_N} G_{M_q}, \quad (14)$$

where $\hat{\mathbf{e}}$ is the spin polarisation vector determined by the choice of polarisation direction of the nucleon.

Utilising ratios of correlators with and without the applied external field, we can define “effective form factors” by appropriate scaling of the effective energy shift $\Delta E_{N\text{eff}}$,

$$G_{E_q(\text{eff.})} = \frac{E_N}{M_N} \frac{\Delta E_{N(\text{eff.})}}{\lambda}, \quad (15)$$

$$G_{M_q(\text{eff.})} = \frac{2E_N}{[\hat{\mathbf{e}} \times \mathbf{q}]_i} \frac{\Delta E_{N(\text{eff.})}}{\lambda_i}. \quad (16)$$

These should plateau to the relevant form factors provided λ is small enough that the energy shift is predominantly linear. Fig. 1 shows results for effective electromagnetic form factors for a subset of Q^2 values. Here we identify that quite clean plateaux are realised up to quite large momentum transfer. As a check on the selected fit window, we ensure that the free-field correlators are sufficiently saturating to the ground-state energy dispersion.

Fig. 2 shows results for the proton electric and magnetic form factors — neglecting disconnected contributions, which are anticipated to be very small at large Q^2 [42]. In the low- Q^2 region we compare with results computed on the same ensembles using a variationally-improved 3-point function approach, as described in [25]. Very good agreement is observed in the region of overlap. The statistical signal for the new Feynman–Hellmann approach is seen to extend to much larger Q^2 than has been accessible in the past.

Phenomenologically, the Q^2 -range we are now able to access would allow for tighter constraints to be placed on the distribution of charge and magnetisation in the nucleon at small impact parameter [43].

Fig. 3 displays the extraction of the ratio G_E/G_M as a function of Q^2 , and a comparison to experiment [5–7]. While nothing definitive can be concluded about a potential zero crossing, the overall trend is seen to compare very well with the experimental data.

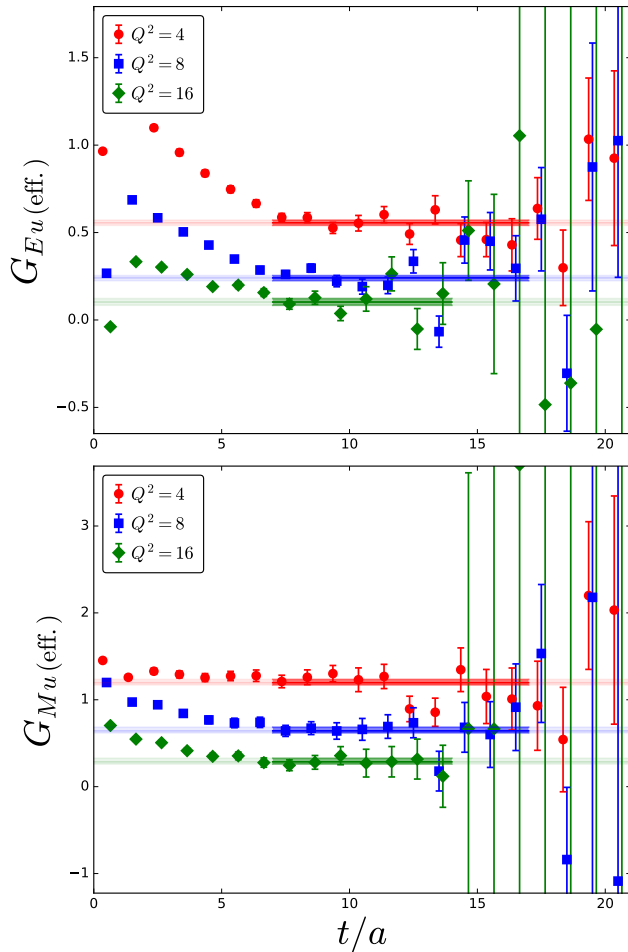


FIG. 1. Effective electric and magnetic form factors of the u quark in the nucleon for different values of Q^2 . Results shown are for a single value of $\lambda \neq 0$ (since we are in the linear region, results at different λ are statistically identical).

B. Electromagnetic Form Factor of the Pion

Following a similar analysis as that for the nucleon, we show the determination of the pion form factor and comparison to experiment [12] in Fig. 4. The realised statistical signal gives confidence that future lattice simulations will be able to provide important insight into this transition between the perturbative and nonperturbative.

V. CONCLUSION

In this work we have extended the Feynman–Hellmann technique to access non-forward matrix elements. We demonstrate that this provides for a dramatic improvement in the ability to extract nucleon and pion form factors at much higher momentum transfers than previously possible. Before making rigorous comparisons with phe-

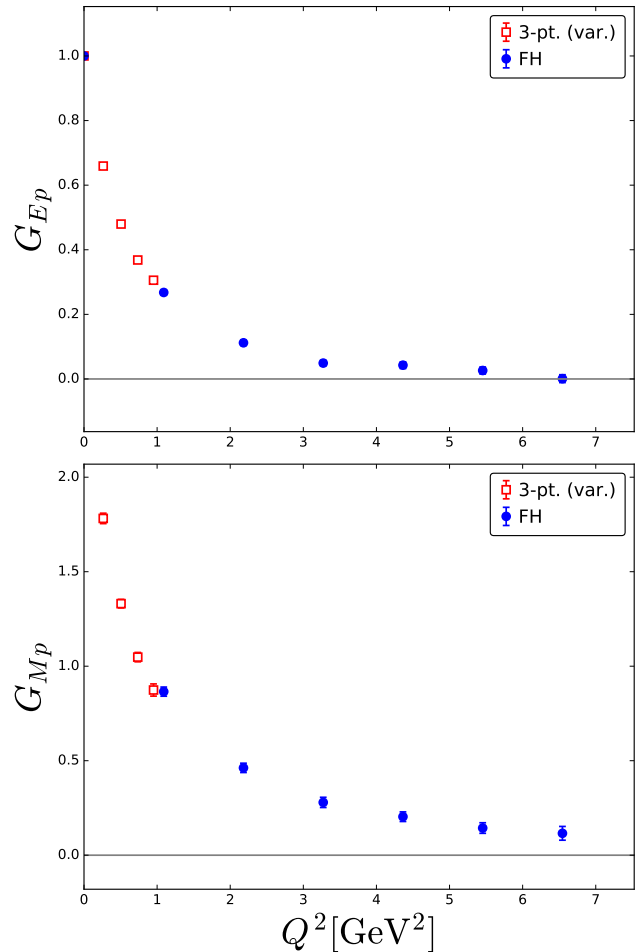


FIG. 2. G_E and G_M for the proton from the Feynman–Hellmann method and a variational method described in [25] employed on the same ensemble.

nomenology, standard lattice systematics must be further quantified, including quark mass dependence, discretisation artifacts and continuum extrapolation. There is also further potential for increased precision by using improved operators that have better access to high-momentum states, as proposed in [44].

The high-momentum form factors extracted in this work demonstrate a significantly expanded scope for lattice QCD to address this phenomenologically interesting domain of hadron structure.

ACKNOWLEDGMENTS

The numerical configuration generation was performed using the BQCD lattice QCD program [45], on the IBM BlueGeneQ using DIRAC 2 resources (EPCC, Edinburgh, UK), the BlueGene P and Q at NIC (Jülich, Germany) and the Cray XC30 at HLRN (Berlin–Hannover, Germany). Some of the simulations were undertaken

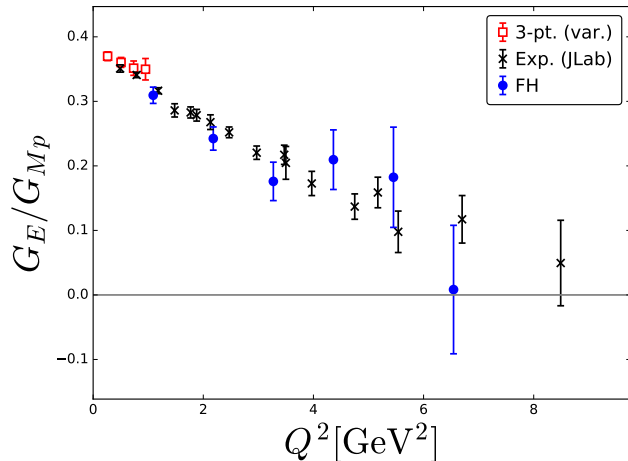


FIG. 3. Ratio G_E/G_M for the proton from application of the Feynman–Hellmann method, from a variational analysis of three-point functions [25], and from experiment [5–7]. Note this is not scaled by the magnetic moment of the proton μ_p , as this would require phenomenological fits to the low Q^2 data, which is not the focus of this work.

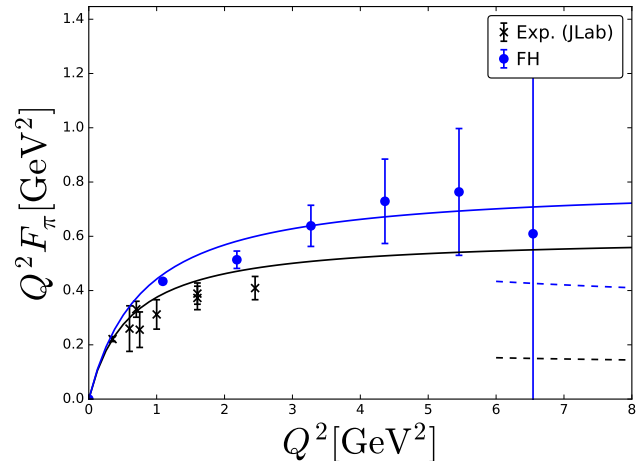


FIG. 4. Scaled pion form factor $Q^2 F_\pi$ from the Feynman–Hellmann technique and from experiment [12]. The solid lines are the vector meson dominance at the relevant pion masses, and the dotted lines are the asymptotic values predicted by perturbative QCD (see [13] for a discussion of this value and its limitations).

using resources awarded at the NCI National Facility in Canberra, Australia, and the iVEC facilities at the Pawsey Supercomputing Centre. These resources are provided through the National Computational Merit Allocation Scheme and the University of Adelaide Partner Share supported by the Australian Government. This work was supported in part through supercomputing resources provided by the Phoenix HPC service at the University of Adelaide. The BlueGene codes were optimised using Bagel [46]. The Chroma software library [47], was used in the data analysis. AC was supported by the Australian Government Research Training Program Scholarship. JD gratefully acknowledges support by the National Superconducting Cyclotron Laboratory (NSCL)/Facility GS was supported by DFG grant SCHI 179/8-1. HP was supported by DFG grant SCHI 422/10-1. for Rare Isotope Beams (FRIB) and Michigan State University (MSU) during the preparation of this work. This investigation has been supported by the Australian Research Council under grants FT120100821, FT100100005 and DP140103067 (RDY and JMZ).

-
- [1] M. N. Rosenbluth, *Phys. Rev.* **79**, 615 (1950).
[2] I. A. Qattan *et al.*, *Phys. Rev. Lett.* **94**, 142301 (2005), arXiv:nucl-ex/0410010 [nucl-ex].
[3] M. K. Jones *et al.* (Jefferson Lab Hall A), *Phys. Rev. Lett.* **84**, 1398 (2000), arXiv:nucl-ex/9910005 [nucl-ex].
[4] O. Gayou *et al.* (Jefferson Lab Hall A), *Phys. Rev. Lett.* **88**, 092301 (2002), arXiv:nucl-ex/0111010 [nucl-ex].
[5] V. Punjabi *et al.*, *Phys. Rev.* **C71**, 055202 (2005), [Erratum: *Phys. Rev.* **C71**, 069902(2005)], arXiv:nucl-ex/0501018 [nucl-ex].
[6] A. J. R. Puckett *et al.*, *Phys. Rev. Lett.* **104**, 242301 (2010), arXiv:1005.3419 [nucl-ex].
[7] A. J. R. Puckett *et al.*, *Phys. Rev.* **C85**, 045203 (2012), arXiv:1102.5737 [nucl-ex].
[8] P. A. M. Guichon and M. Vanderhaeghen, *Phys. Rev. Lett.* **91**, 142303 (2003), arXiv:hep-ph/0306007 [hep-ph].
[9] P. G. Blunden, W. Melnitchouk, and J. A. Tjon, *Phys. Rev.* **C72**, 034612 (2005), arXiv:nucl-th/0506039

- [nucl-th].
- [10] J. Volmer *et al.* (Jefferson Lab F(pi)), Phys. Rev. Lett. **86**, 1713 (2001), arXiv:nucl-ex/0010009 [nucl-ex].
- [11] T. Horn *et al.* (Jefferson Lab F(pi)-2), Phys. Rev. Lett. **97**, 192001 (2006), arXiv:nucl-ex/0607005 [nucl-ex].
- [12] G. M. Huber *et al.* (Jefferson Lab), Phys. Rev. **C78**, 045203 (2008), arXiv:0809.3052 [nucl-ex].
- [13] L. Chang *et al.*, Phys. Rev. Lett. **111**, 141802 (2013), arXiv:1307.0026 [nucl-th].
- [14] T. Horn and C. D. Roberts, J. Phys. **G43**, 073001 (2016), arXiv:1602.04016 [nucl-th].
- [15] S. Collins *et al.*, Phys. Rev. **D84**, 074507 (2011), arXiv:1106.3580 [hep-lat].
- [16] C. Alexandrou, M. Brinet, J. Carbonell, M. Constantinou, P. A. Harraud, P. Guichon, K. Jansen, T. Korzec, and M. Papinutto, Phys. Rev. **D83**, 094502 (2011), arXiv:1102.2208 [hep-lat].
- [17] P. E. Shanahan, A. W. Thomas, R. D. Young, J. M. Zanotti, R. Horsley, Y. Nakamura, D. Pleiter, P. E. L. Rakow, G. Schierholz, and H. Stben (QCDSF/UKQCD, CSSM), Phys. Rev. **D89**, 074511 (2014), arXiv:1401.5862 [hep-lat].
- [18] P. E. Shanahan, A. W. Thomas, R. D. Young, J. M. Zanotti, R. Horsley, Y. Nakamura, D. Pleiter, P. E. L. Rakow, G. Schierholz, and H. Stben, Phys. Rev. **D90**, 034502 (2014), arXiv:1403.1965 [hep-lat].
- [19] J. R. Green, J. W. Negele, A. V. Pochinsky, S. N. Syritsyn, M. Engelhardt, and S. Krieg, Phys. Rev. **D90**, 074507 (2014), arXiv:1404.4029 [hep-lat].
- [20] S. Capitani, M. Della Morte, D. Djukanovic, G. von Hippel, J. Hua, B. Jger, B. Knippschild, H. B. Meyer, T. D. Rae, and H. Wittig, Phys. Rev. **D92**, 054511 (2015), arXiv:1504.04628 [hep-lat].
- [21] H.-W. Lin, S. D. Cohen, R. G. Edwards, K. Orginos, and D. G. Richards, (2010), arXiv:1005.0799 [hep-lat].
- [22] J. Koponen, A. C. Zimmermann-Santos, C. T. H. Davies, G. P. Lepage, and A. T. Lytle, (2017), arXiv:1701.04250 [hep-lat].
- [23] B. J. Owen, J. Dragos, W. Kamleh, D. B. Leinweber, M. S. Mahbub, B. J. Menadue, and J. M. Zanotti, Phys. Lett. **B723**, 217 (2013), arXiv:1212.4668 [hep-lat].
- [24] B. Yoon *et al.*, Phys. Rev. **D93**, 114506 (2016), arXiv:1602.07737 [hep-lat].
- [25] J. Dragos, R. Horsley, W. Kamleh, D. B. Leinweber, Y. Nakamura, P. E. L. Rakow, G. Schierholz, R. D. Young, and J. M. Zanotti, Phys. Rev. **D94**, 074505 (2016), arXiv:1606.03195 [hep-lat].
- [26] R. Horsley, R. Mollo, Y. Nakamura, H. Perlt, D. Pleiter, P. E. L. Rakow, G. Schierholz, A. Schiller, F. Winter, and J. M. Zanotti (UKQCD, QCDSF), Phys. Lett. **B714**, 312 (2012), arXiv:1205.6410 [hep-lat].
- [27] A. J. Chambers *et al.* (QCDSF/UKQCD, CSSM), Phys. Rev. **D90**, 014510 (2014), arXiv:1405.3019 [hep-lat].
- [28] A. J. Chambers, R. Horsley, Y. Nakamura, H. Perlt, P. E. L. Rakow, G. Schierholz, A. Schiller, and J. M. Zanotti (QCDSF), Phys. Lett. **B740**, 30 (2015), arXiv:1410.3078 [hep-lat].
- [29] A. J. Chambers *et al.*, Phys. Rev. **D92**, 114517 (2015), arXiv:1508.06856 [hep-lat].
- [30] W. Detmold, Phys. Rev. **D71**, 054506 (2005), arXiv:hep-lat/0410011 [hep-lat].
- [31] M. Engelhardt (LHPC), Phys. Rev. **D76**, 114502 (2007), arXiv:0706.3919 [hep-lat].
- [32] W. Detmold, B. C. Tiburzi, and A. Walker-Loud, Phys. Rev. **D79**, 094505 (2009), arXiv:0904.1586 [hep-lat].
- [33] W. Detmold, B. C. Tiburzi, and A. Walker-Loud, Phys. Rev. **D81**, 054502 (2010), arXiv:1001.1131 [hep-lat].
- [34] T. Primer, W. Kamleh, D. Leinweber, and M. Burkardt, Phys. Rev. **D89**, 034508 (2014), arXiv:1307.1509 [hep-lat].
- [35] W. Freeman, A. Alexandru, M. Lujan, and F. X. Lee, Phys. Rev. **D90**, 054507 (2014), arXiv:1407.2687 [hep-lat].
- [36] M. J. Savage, P. E. Shanahan, B. C. Tiburzi, M. L. Wagman, F. Winter, S. R. Beane, E. Chang, Z. Davoudi, W. Detmold, and K. Orginos, (2016), arXiv:1610.04545 [hep-lat].
- [37] C. Bouchard, C. C. Chang, T. Kurth, K. Orginos, and A. Walker-Loud, (2016), arXiv:1612.06963 [hep-lat].
- [38] R. Horsley, J. Najjar, Y. Nakamura, H. Perlt, D. Pleiter, P. E. L. Rakow, G. Schierholz, A. Schiller, H. Stben, and J. M. Zanotti (QCDSF-UKQCD), PoS **LATTICE2013**, 249 (2013), arXiv:1311.5010 [hep-lat].
- [39] V. G. Bornyakov *et al.*, (2015), arXiv:1508.05916 [hep-lat].
- [40] W. Bietenholz *et al.*, Phys. Lett. **B690**, 436 (2010), arXiv:1003.1114 [hep-lat].
- [41] W. Bietenholz *et al.*, Phys. Rev. **D84**, 054509 (2011), arXiv:1102.5300 [hep-lat].
- [42] J. Green, S. Meinel, M. Engelhardt, S. Krieg, J. Laeuchli, J. Negele, K. Orginos, A. Pochinsky, and S. Syritsyn, Phys. Rev. **D92**, 031501 (2015), arXiv:1505.01803 [hep-lat].
- [43] S. Venkat, J. Arrington, G. A. Miller, and X. Zhan, Phys. Rev. **C83**, 015203 (2011), arXiv:1010.3629 [nucl-th].
- [44] G. S. Bali, B. Lang, B. U. Musch, and A. Schäfer, Phys. Rev. **D93**, 094515 (2016), arXiv:1602.05525 [hep-lat].
- [45] Y. Nakamura and H. Stüben, PoS **LATTICE2010**, 040 (2010), arXiv:1011.0199 [hep-lat].
- [46] P. A. Boyle, Comput. Phys. Commun. **180**, 2739 (2009).
- [47] R. G. Edwards and B. Joo (SciDAC, LHPC, UKQCD), Nucl. Phys. Proc. Suppl. **140**, 832 (2005), arXiv:hep-lat/0409003 [hep-lat].